Detecting and Evaluating the Effect of Overlaying Thin Cirrus Cloud on MODIS Retrieved Water-Cloud Droplet Effective Radius

F.-L Chang and Z. Li
Earth System Science Interdisciplinary Center
University of Maryland
College Park, Maryland

Z. Li
Department of Meteorology
University of Maryland
College Park, Maryland

Introduction

Cirrus clouds can largely modify the solar reflected and terrestrial emitted radiances. The ubiquitous presence of cirrus clouds has a global coverage of about 20% to30% and more than 70% in the tropics (Wylie et al. 1994). The probability of cirrus clouds overlaying a low-level boundary layer cloud system is greater than 50% (Hahn et al. 1982, 1984; Tian and Curry 1989; Mace et al. 1997). They are often optically thin and semitransparent and frequently reside in high altitude overlapping with a low-level cloud system. With the high probability of cirrus contamination in satellite imagery data, boundary layer cloud microphysical properties, like droplet effective radius (DER), retrieved from satellite radiance measurements are likely to be biased.

Satellite measurements at 3.7-μm from the advanced very high resolution radiometer (AVHRR) have been widely used to retrieve DER for boundary-layer water clouds. However, uncertainty arises from the influence of thin cirrus contamination because ice particles have distinct optical properties from those of water droplets. Not only are solar reflectance measurements modified by high-altitude cirrus particles, but the 3.7-μm thermal emission may also be affected, which must be properly accounted for in the retrieval processes. Little attention has been paid to characterizing the effects of cirrus contamination on the DER retrievals, due to insufficient spectral information. Now, the moderate-resolution imaging spectroradiometer (MODIS) provides 36-channel high spectral resolution data that greatly enhance our capability of detecting thin cirrus clouds and examining their potential effects on the DER retrievals (King et al. 1992; 2003). Case studies are presented here using MODIS data to investigate the potential effects of thin cirrus contamination on the water-dominant cloud DER retrieved from MODIS 3.7-μm, 2.1-μm, and 1.6-μm measurements, respectively.

The investigation is based on comparisons of DER retrievals for pixels with and without cirrus contamination. Two different methods, namely, the CO_2-slicing algorithm and a conventional 11-μm retrieval method, are used to determine the presence of cirrus clouds.

Data

The MODIS imager carried 36 channels between 0.415-14.2 μm (King et al. 1992) with a nominal spatial resolution of 1 km at nadir (250 m for channels 1 and 2 and 500 m for channels 3-7). The MODIS Level-1B 1-km Calibrated Earth View Data Products are used in this study. In Level-1B 1-km data, radiance measurements at the 250-m and 500-m resolution bands are aggregated to 1-km resolution (MCST 2000). For cloud detection, the MODIS cloud mask algorithms were applied to Level-1B data at nearly half of the 36 channels (Ackerman et al. 1997). Aside from the cloud mask products, separate products of cloud top properties (including height, temperature, and emissivity) were generated over 5 pixels × 5 pixels using the MODIS CO_2 slicing algorithm (Menzel et al. 2002). The cloud water phase was determined based on an infrared algorithm by comparing the brightness temperature differences at 8.6 μm, 11 μm, and 12 μm (Menzel et al. 2002), which was supplemented by a solar reflection function technique during daytime (King et al. 1997).

Comparison of MODIS CO_2-Slicing and 11-μm Cloud-Top Temperatures

In estimating the effective cloud-top temperature, previous studies (e.g., using the AVHRR data) have utilized the 11-μm emission temperature to determine cloud-top temperature (e.g., Han et al. 1994; Platnick and Twomey 1994; Nakajima and Nakajima 1995). In the MODIS DER retrieval, a single cloud-top temperature at a spatial resolution of 25 km^2 was estimated by the CO_2-slicing algorithm (Menzel et al. 2002). The MODIS CO_2-slicing algorithms employed four MODIS infrared channels in the CO_2 absorption bands (i.e., 13.3, 13.6, 13.9, and 14.2 μm). The CO_2-slicing method is known for its effectiveness in detecting high-level thin cirrus clouds, noting that the high-level thin cirrus clouds are often transparent at the 11-μm channel. Thus, the CO_2-slicing derived cloud-top temperature will be smaller than the 11-μm retrieved cloud-top temperature for a thin cirrus cloud overlaying over an optically-thick low-level cloud.

Figure 1 shows a comparison of cloud-top temperatures retrieved using the CO_2-slicing method and the 11-μm emission measurements for the MODIS water-dominant cloudy pixels. Although the two retrieved temperatures are generally greater than 273 K, the CO_2-slicing cloud-top temperatures are much colder than the 11-μm cloud-top temperatures. A most likely cause is the extra-sensitivity of the CO_2-slicing technique to cloud-top altitude, even though an overwhelming amount of radiance originated from the thicker low-level clouds. Consequently, the significantly colder cloud-top skin temperature detected by the CO_2-slicing method relative to 11-μm cloud-top temperatures can be used to detect cirrus-contaminated water-cloud pixels when high-level thin cirrus clouds are present.

Comparisons of Droplet Effective Radius Retrieved from MODIS

To examine the effect of cirrus contamination on the DER retrievals, a threshold value of 3 K between the CO_2-slicing and the 11-μm cloud-top temperatures was used to separate cirrus-contaminated from no-cirrus contaminated pixels for the water-cloud pixels identified by MODIS. Figure 2 shows the

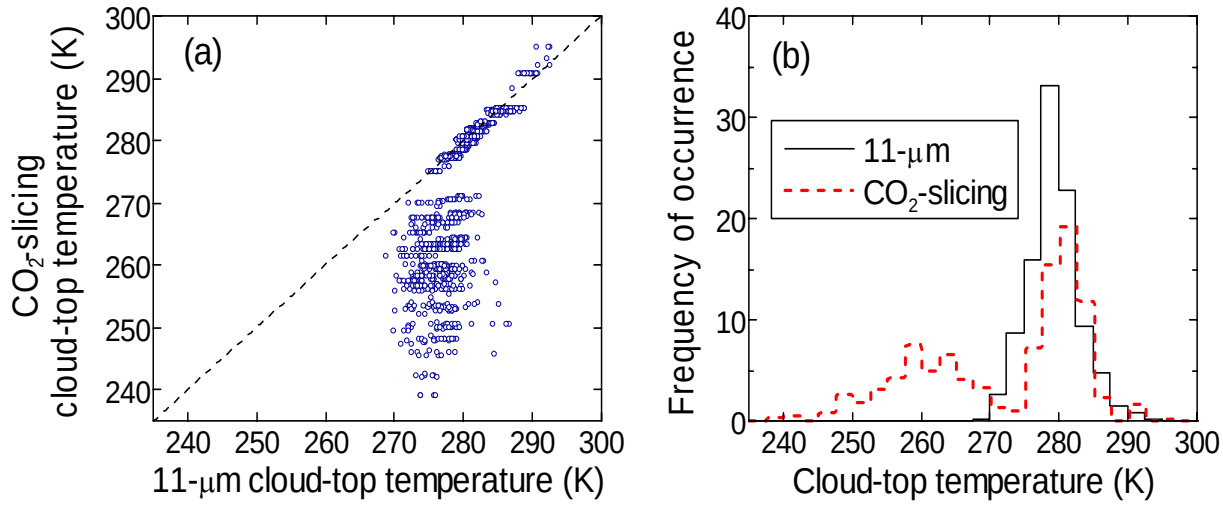

Figure 1. (a) Cloud-top temperatures retrieved from the CO_2-slicing method and the 11-μm channel. (b) Frequency distributions of the two cloud-top temperatures.

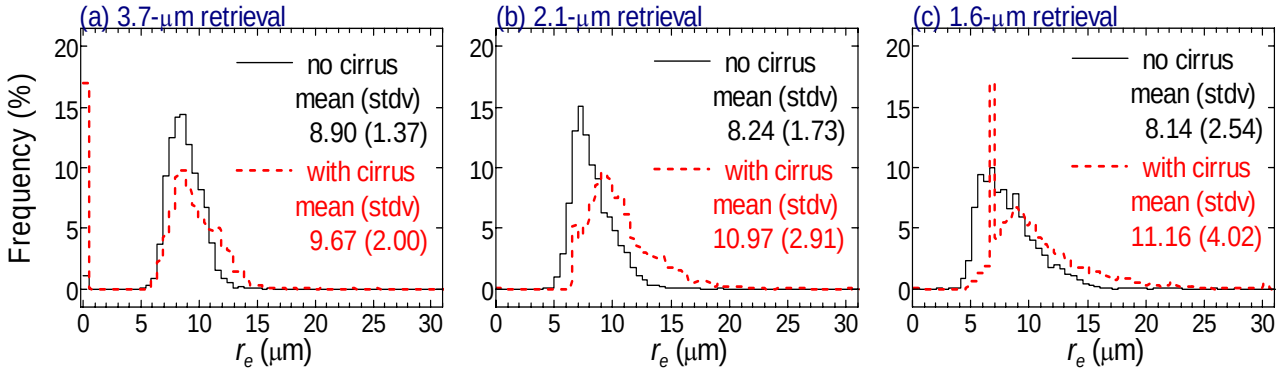

Figure 2. Frequency distributions of the MODIS DER retrievals for water clouds with cirrus (red) and without cirrus contamination (black). Results are obtained from a (100 km^2) area on April 2, 2001.

comparisons of the DER retrievals between cirrus-free and cirrus-contaminated water clouds using the MODIS 3.7-μm, 2.1-μm, and 1.6-μm measurements obtained on April 2, 2001, from a (100 km^2) area over Oklahoma. The retrieved mean DER for cirrus-free water clouds are 8.90 (±1.37) μm, 8.24 (± 1.73) μm, and 8.14 (±2.54) μm for the 3.7-μm, 2.1-μm, and 1.6-μm retrievals, respectively. In contrast, the mean DER for the water clouds contaminated by cirrus were 9.67 (±2.00) μm (at 3.7-μm), 10.97 (±2.91) μm (at 2.1-μm) and 11.16 (±4.02) μm (at 1.6-μm), respectively. A progressive overestimation of DER for cirrus contaminated pixels from 3.7-μm to 1.6-μm were attributed to the increased absorption differences between ice particles and water droplets. Note that for non-cirrus

contaminated water clouds, the difference in the three DER retrievals indicates changes of the DER from cloud top to cloud base (e.g., Miles et al. 2002).

Simulations from Theoretical Model

Two different non-spherical ice crystal models with distinct optical properties were adopted from Yang and Liou (1996a, b) to simulate the radiative effects of thin cirrus clouds overlapping with a low-level water cloud layer. The two different cirrus models were computed at the MODIS channels using an improved geometric ray-tracing/Monte Carlo method and a finite-difference time domain method for different size parameters. Figure 3 illustrates the model simulated cirrus effects on the DER retrievals and cloud-top emission temperatures. Figure 3a shows the cirrus effects on the DER retrievals at 3.7, 2.1, and 1.6 μm and Figure 3b shows the effects on modifying the brightness temperatures at 3.7 and 11 μm, respectively. The first cirrus model is associated with an effective size of 12.7 μm, which is non-absorbing at visible wavelengths like the water cloud, but is more absorbing than the water cloud at longer near-IR wavelengths; the second cirrus model has an effective size of 53.3 μm, which has a much larger absorption than does the other cirrus model. It is clear that the second cirrus model has a larger influence on the retrievals than the first cirrus model. Depending on the absorption strength of cirrus particles and the optical depth, significant overestimation may occur in all three DER retrievals except for one case at 3.7 μm (cf. Figure3a). This is because the cirrus cloud has a larger effect in reducing the emission temperatures at 11-μm than at 3.7-μm (cf. Figure 3b). Because conventionally the 11-μm emission temperature was used to account for the 3.7-μm thermal emission, the cirrus-reduced 11-μm emission temperatures can thus result in a smaller DER retrieval at 3.7 μm, while a larger DER retrieval occurs at either 2.1-μm or 1.6-μm.

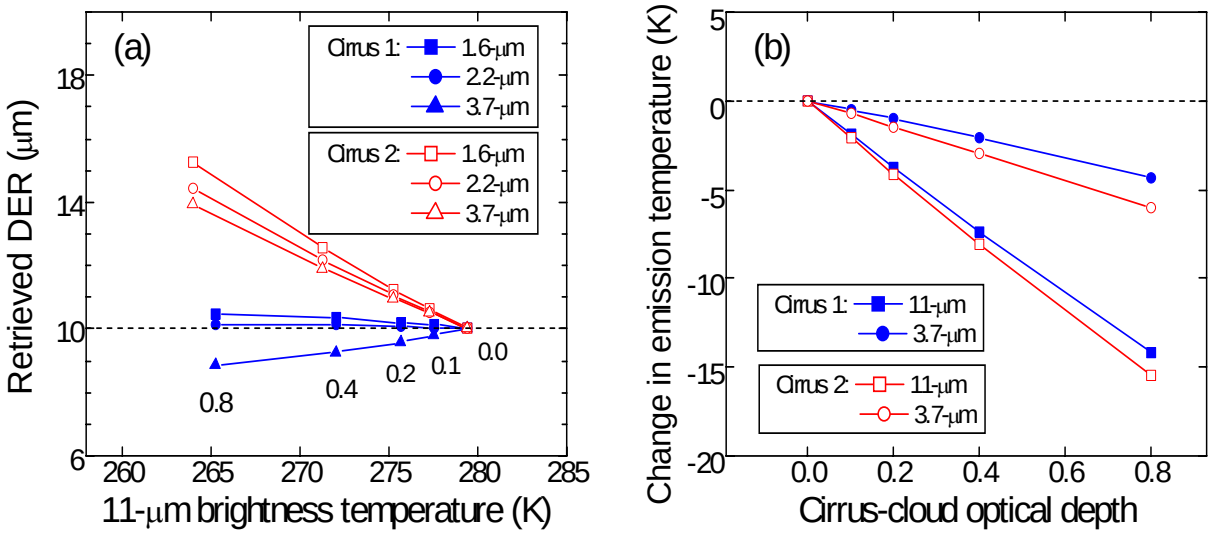

Figure 3. (a) Model simulations of changes in DER retrievals due to various cirrus cloud (optical depth = 0.0-0.8) overlying the low water cloud (r_e =10 μm); (b) Similar to (a) except for cloud-top temperature changes at 3.7 and 11 μm.

Conclusions

Satellite observations from the MODIS can be used to detect thin cirrus clouds overlaying low-level water clouds. It was demonstrated that the differences in cloud-top temperatures retrieved using the MODIS CO_2-slicing algorithm and the conventional 11-μm retrieval method can be indicative of whether a low-level water cloud pixel was contaminated by a high-level cirrus cloud. The effects of thin cirrus clouds on satellite retrieved water-cloud DER were illustrated by comparing the retrievals derived from the MODIS 1.6-μm, 2.1-μm, and 3.7-μm radiance measurements.

Because water droplets and ice particles have different absorbing properties in the near infrared wavelengths, the contamination of cirrus clouds in satellite measurements generally causes overestimation in the retrievals of low-level water-cloud DER using near-infrared measurements, such as 3.7, 2.1, and 1.6 μm. The overestimation was generally greater than 2.5 μm and largest for the 1.6-μm retrieval (with a mean bias ~3 μm) due to the largest difference in the absorption between water droplets and ice particles. The thin cirrus may also have an adverse effect on underestimating the DER retrieval at 3.7 μm resulted from an attenuation effect in the thermal emission that also contributed to the 3.7-μm measurements.

Acknowledgement

This work was supported by the U.S. Department of Energy Grant No. DE-FG02-97ER62361 under the Atmospheric Radiation Measurement (ARM) Program.

Corresponding Author

Fu-Lung Chang, fchang@essic.umd.edu, (301) 405-5568

References

Ackerman, S., et al., 1997: Discriminating clear-sky from cloud. MODIS Algorithm Theoretical Basis Document No. ATBD-MOD-06, p. 105.

Hahn, C. J., and Coauthors, 1982: Atlas of simultaneous occurrence of different cloud types over the ocean. NCAR Tech. Note, TN241 + STR, p. 209. Available from National Center for Atmospheric Research, Boulder, Colorado.

Hahn, C. J., S. G. Warren, J. London, R. M. Chervin, and R. Jenne, 1984: Atlas of simultaneous occurrence of different cloud types over land. NCAR Tech. Note TN-241 + STR, p. 216. Available from National Center for Atmospheric Research, Boulder, Colorado.

Han, Q., W. B. Rossow, and A. A. Lacis, 1994: Near-global survey of effective droplet radii in liquid water clouds using ISCCP data. *J. Climate*, **7**, 465-497.

King, M. D., Y. J. Kaufman, W. P. Menzel, and D. Tanre, 1992: Remote-sensing of cloud, aerosol, and water-vapor properties from the moderate-resolution imaging spectrometer (MODIS). *IEEE Trans. Geosci. Remote Sensing*, **30**, 2-27.

King, M. D., S.-C. Tsay, S. E. Platnick, M. Wang, and K.-N. Liou, 1997: Cloud retrieval algorithms for MODIS: Optical thickness, effective particle radius, and thermodynamic phase. MODIS Algorithm Theoretical Basis Document No. ATBD-MOD-06 Cloud product, p 83.

King, M. D., W. P. Menzel, Y. J. Kaufman, D. Tanre, B. C. Gao, S. Platnick, S. A. Ackerman, L. A. Remer, R. Pincus, and P. A. Hubanks, 2003: Cloud and aerosol properties, precipitable water, and profiles of temperature and humidity from MODIS. *IEEE Trans. Geosci. Remote Sens.*, in press.

Mace, G. G., T. P. Ackerman, and E. E. Clothiaux, 1997: A study of composite cirrus morphology using data from a 94-GHz radar and correlation with temperature and large-scale vertical motion. *J. Geophys. Res.*, **102**, 13,581-13,593.

Menzel, W. P., B. A. Baum, K. I. Strabala, and R. A. Frey, 2002: Cloud-top properties and cloud phase. MODIS Algorithm Theoretical Basis Document, ATBD-MOD-07, p. 61.

Miles, N. L., J. Verlinde, and E. E. Clothiaux, 2000: Cloud droplet size distributions in low-level stratiform clouds. *J. Atmos. Sci.*, **57**, 295-311.

Nakajima, T. Y., and T. Nakajima, 1995: Wide-area determination of cloud microphysical properties from NOAA AVHRR measurements for FIRE and ASTEX regions. *J. Atmos. Sci.*, **52**, 4043-4059.

Platnick, S., and S. Twomey, 1994: Determining the susceptibility of cloud albedo to changes in droplet concentrations with the advanced very high resolution radiometer. *J. Appl. Meteorol.*, **33**, 334-347.

Tian, L., and J. A. Curry, 1989: Cloud overlap statistics. *J. Geophys. Res.*, **94**, 9925-9935.

Wylie, D. P., W. P. Menzel, H. M. Woolf, and K. I. Strabala, 1994: Four years of global cirrus cloud statistics using HIRS. *J. Climate*, **7**, 1972-1986.

Yang, P., and K.-N. Liou, 1996a: Finite-difference time domain method for light scattering by small ice crystals in three-dimensional space. *J. Opt. Soc. Am.*, **13**, 2072-2085.

Yang, P., and K.-N. Liou, 1996b: Geometric optics integral equation method for light scattering by nonspherical ice crystals. *Appl. Opt.*, **35**, 6568-6584.